2005 American Control Conference
June 8-10, 2005. Portland, OR, USA

Design of an Optimal Clutch Controller for Commercial Trucks

James David and Narasimhamurthi Natarajan

Abstract— **This paper describes a procedure to determine the parameters of well established driveline models using signals that are readily available on the vehicle data bus. Experimental results performed on a class 6 commercial truck are provided and the quality of the model fidelity is discussed. Two control strategies based on LQR technique are discussed to illustrate automatic selection of controller structure and controller parameters. The first technique permits large initial torque which may be desirable when launching up a slope. The second technique enforces smooth clutch-torque profile to ensure driver comfort. The parameter estimation procedure can be easily incorporated as part of regular maintenance to ensure the controller performance do not deteriorate over a period of time. Thus, when the procedure described in the paper is implemented, the driver will have the ability to select the quality of the launch described by features such as power dissipation, longitudinal acceleration etc. Simulation results, using the described procedure taking into account the torque-speed characteristics of the engine and the typical load on the vehicle, are presented and discussed.**

I. INTRODUCTION

Automatic control of clutches for vehicle start up and smooth shifting has been an important area of research among powertrain components and systems manufacturers for a number of years. With the surge in the development and use of system simulation tools, complimented by vastly improved electronics in the last 20 years, automated clutch systems are now available in numerous configurations at an affordable prices. Some of the obvious advantages for implementing automatic clutch control are 1: Improved driver comfort by eliminating the clutch pedal, hence have only two pedal operation. 2: Ease of vehicle launch on gradients. 3: Improved clutch life because of intelligent clutch abuse prevention logic 4: Reducing driveline noise and vibration at low speed by tightly controlling the slip speed. In addition different clutch engagement profiles can be provided to suit various driving styles.

II. BACKGROUND LITERATURE

Several control strategies of clutch engagements have been proposed to realize vehicle start up. Tanaka *et al* [1] proposed engaging the clutch in proportion to the engine speed. However this method could be susceptible to inconsistent launch characteristics due to variation in clutch friction coefficient. For designing a controller based on typical driver's start up operation, Sumida *et al* [2] investigated the driver's clutch operation using a series of controlled driver response tests. He concluded that engine sound feedback, which relates to engine speed, was critical information for optimum clutch operation. The stated advantages of this control scheme were engine output torque tracking with throttle pedal position and consistent performance against engine torque and clutch friction variation. Clutch engagement with and without throttle, and its optimization has been investigated in detail by Szadkowski *et al* [3], [4]. He defines an ideal engagement as an engagement with constant plate loading rate, so as to minimize the engagement time, while satisfying the no-vehicle-lurch and no engine-kill criterion. Nordgard *et al* [5] has proposed adaptive routines in the clutch control algorithm that compensates for sensor drift and provides different engagement feel depending on the driving style.

Fuzzy logic has been successfully employed by Tanaka *et al* [6]. Based on the engagement requirements, a control law for clutch engagement is established and membership functions of clutch release lever position along with accelerator pedal position and engine rotational speeds are used to calculate the incremental engaging or disengaging displacement. Wu *et al* [7] has analyzed the stability of the fuzzy controller, using linear approximation to Lyapunov's stability criterion and applying the asymptotic stability principle. A range of values for the input, linearized with respect to the dependent variables, are obtained. By ensuring the control state is within this stable range, control objectives were successfully achieved.

In order to overcome the performance limitations of linear control strategies for highly nonlinear systems, Chen *et al* [8], converted a non-linear dynamic clutch model into linearized system using submanifold transforms. A much closer match with the ideal response with improved robustness is obtained for the feedback linearized case, compared to direct control of the non-linear clutch system. Hibino *et al* [9] has implemented robust control method to ensure stability against variations of the clutch characteristics by using disturbance attenuation filters. Robust clutch control has also been demonstrated by Slicker *et al* [10], using quantitative feedback theory.

Optimal control techniques have been used by Glielmo *et al* [11] and Garofalo *et al* [12] to control the engagement of dry clutch, where the objective function to be minimized consists of separately weighted squared terms of slip speed and the control input.

This paper first discuses the parameter estimation of a simple driveline model. Two clutch engagement strategies based on LQR methods are then developed. In addition to using only the slip speed and control input in the performance index as has been done in the past, clutch

James David is a Lead Engineer, Controls Systems, Advanced Powertrain Group, Eaton Corporation, Southfield, MI 48076, USA jamesdavid@eaton.com

Dr. N. Natarajan is with the faculty in the Department of Electrical Engineering, The University of Michigan, Dearborn, MI 48435, USA nnarasim@engin.umd.umich.edu

power and slip acceleration are also weighted. This results in a procedure that provides tunable parameters to realize various types of clutch engagement ranging from performance to comfort driven vehicle launch quality.

III. Driveline Model

A model of the driveline is required for developing various clutch control schemes efficiently and accurately. For this study, a model that captures the first resonance modes and thereby explains the major oscillations in the engine, transmission and wheel speeds, is sufficient for the purposes of the controller development. The target application is a single axle rear wheel drive medium duty, class 6 truck. This driveline consists of the engine and flywheel, clutch, transmission, propeller shaft, axle, drive shaft and the wheels. Each of these components is treated as a sub-system and Newtonian equations are used to describe the component dynamics. The components themselves are either modeled as a stiff shaft which transmits torque without any torsional deflection, or as rotating inertias connected by flexible shafts having internal structural damping. This model is derived from models proposed by Pettersson [13]. The model assumes a flexible drive shaft, which is the only compliant member in the driveline.

A. System Level Description

The complete set of equations that describe the driveline dynamics for the slipping clutch model and the locked clutch model can be written as follows.[1]

a) Slipping Clutch Model:

$$J_e\ddot{\alpha_e} = T_e - T_c - b_e\dot{\alpha_e} \tag{1}$$

$$\left(\frac{J_t}{n_t^2}+\frac{J_f}{n^2}\right)\ddot{\alpha_c} = T_c - \left(\frac{b_t}{n_t^2}+\frac{b_f}{n^2}\right)\dot{\alpha_c} - \frac{K_a}{n}\left(\frac{\alpha_c}{n}-\alpha_w\right) - \frac{b_a}{n}\left(\frac{\dot{\alpha_c}}{n}-\dot{\alpha_w}\right) \tag{2}$$

$$\left(J_w + mr_w^2\right)\ddot{\alpha_w} = K_a\left(\frac{\alpha_c}{n}-\alpha_w\right) + b_a\left(\frac{\dot{\alpha_c}}{n}-\dot{\alpha_w}\right) - \left(b_w + mc_{r2}r_w^2c_{r2}\right)\dot{\alpha_w} - mr_w\left(c_{r1}+g\sin\xi\right) \tag{3}$$

b) Locked Clutch Model:

$$\left(J_e+\frac{J_t}{n_t^2}+\frac{J_f}{n^2}\right)\ddot{\alpha_c} = T_e - \left(b_e+\frac{b_t}{n_t^2}+\frac{b_f}{n^2}\right)\dot{\alpha_c} - \frac{K_a}{n}\left(\frac{\alpha_c}{n}-\alpha_w\right) - \frac{b_a}{n}\left(\frac{\dot{\alpha_c}}{n}-\dot{\alpha_w}\right) \tag{4}$$

$$\left(J_w + mr_w^2\right)\ddot{\alpha_w} = K_a\left(\frac{\alpha_c}{n}-\alpha_w\right) + b_a\left(\frac{\dot{\alpha_c}}{n}-\dot{\alpha_w}\right) - \left(b_w + mc_{r2}r_w^2c_{r2}\right)\dot{\alpha_w} - mr_w\left(c_{r1}+g\sin\xi\right) \tag{5}$$

[1] List of symbols are found in appendix

B. State Space Representation

The next step is to develop a state space representation of both the slipping and locked clutch systems. The slipping system is considered first. Choosing the following state variables,

$$x_1 = \dot{\alpha_e} \qquad x_2 = \left(\frac{\alpha_c}{n}-\alpha_w\right)$$
$$x_3 = \dot{\alpha_c} \qquad x_4 = \dot{\alpha_w}$$
$$n = n_t n_f$$

Inserting these in (1), (2) and (3), the following state space matrices are obtained.

$$\mathbf{A_s} = \begin{pmatrix} -\frac{b_e}{J_0} & 0 & 0 & 0 \\ 0 & 0 & \frac{1}{n} & -1 \\ 0 & -\frac{K_a}{nJ_1} & -\frac{1}{J_1}\left(b_1+\frac{b_a}{n^2}\right) & \frac{b_a}{nJ_1} \\ 0 & \frac{K_a}{J_2} & \frac{b_a}{nJ_2} & -\frac{1}{J_2}\left(b_a+b_2\right) \end{pmatrix}$$

$$\mathbf{B_s} = \begin{pmatrix} \frac{1}{J_0} & -\frac{1}{J_0} & 0 \\ 0 & 0 & 0 \\ 0 & \frac{1}{J_1} & 0 \\ 0 & 0 & -\frac{1}{J_2} \end{pmatrix} \qquad \mathbf{U_s} = \begin{pmatrix} T_e \\ T_c \\ T_l \end{pmatrix}$$

$$\mathbf{X_s} = \begin{pmatrix} \dot{\alpha_e} \\ \left(\frac{\alpha_c}{n}-\alpha_w\right) \\ \dot{\alpha_c} \\ \dot{\alpha_w} \end{pmatrix} \tag{6}$$

Similarly, the state space equations for the locked clutch model can be easily developed. Choosing the following state variables,

$$x_1 = \dot{\alpha_e} \qquad x_2 = \left(\frac{\alpha_e}{n}-\alpha_w\right)$$
$$x_3 = \dot{\alpha_w}$$

and inserting into (4) and (5), the following state space matrices are obtained.

$$\mathbf{A_l} = \begin{pmatrix} -\frac{1}{\acute{J}_1}\left(\acute{b}_1+\frac{b_a}{n^2}\right) & -\frac{K_a}{n\acute{J}_1} & -\frac{b_a}{n\acute{J}_1} \\ \frac{1}{n} & 0 & -1 \\ \frac{b_a}{nJ_2} & \frac{K_a}{J_2} & -\frac{1}{J_2}\left(b_a+b_2\right) \end{pmatrix}$$

$$\mathbf{B_l} = \begin{pmatrix} \frac{1}{\acute{J}_1} & 0 \\ 0 & 0 \\ 0 & -\frac{1}{J_2} \end{pmatrix} \qquad \mathbf{U_l} = \begin{pmatrix} T_e \\ T_l \end{pmatrix}$$

$$\mathbf{X_l} = \begin{pmatrix} \dot{\alpha_e} \\ \left(\frac{\alpha_e}{n}-\alpha_w\right) \\ \dot{\alpha_w} \end{pmatrix} \tag{7}$$

In (6) and (7), the following substitutions have been made.

$$J_0 = J_e \qquad b_1 = \frac{b_t}{n_t^2}+\frac{b_f}{n^2}$$
$$J_1 = \frac{J_t}{n_t^2}+\frac{J_f}{n^2} \qquad \acute{b}_1 = b_e+\frac{b_t}{n_t^2}+\frac{b_f}{n^2}$$
$$\acute{J}_1 = J_e+\frac{J_t}{n_t^2}+\frac{J_f}{n^2} \qquad b_2 = b_w + mc_{r2}r_w^2$$
$$J_2 = J_w + mr_w^2 \qquad T_l = mr_w\left(c_{r1}+g\sin\xi\right)$$

IV. Parameter Estimation

To design a controller for a vehicle it is important to obtain values of the parameters in (6) and (7). However experimentally determining the parameters for the slipping clutch is not feasible. On the other hand, it is possible to obtain parameters for the locked clutch and use these results to design a controller for launch (slipping clutch).

A. Experiments

The experiment consisted of obtaining the system driveline response to step torque inputs. This was carried out by first launching the vehicle and after the clutch is locked, applying step throttle inputs to the driveline and measuring engine torque, wheel and engine speeds. Maximum energy is transmitted into the driveline by step inputs and additionally, in first gear, the torque multiplication at the wheels is the highest, resulting in exciting various vibration modes with rich frequency content and amplitudes.

B. Instrumentation

The target truck was a medium duty class 6 commercial truck with the following specifications:

- Engine: Cummins IBT
- Transmission: Eaton 6 speed auto shift
- Propshaft: 1810, 3 in series
- Axle: Rockwell, 4.73 final drive ratio
- Tires: Goodyear 22, dual tires
- GVW: 17,000lbs

This truck is equipped with CAN bus connecting CAN-nodes, which among other variables, broadcasts engine torque, friction torque, engine map, engine speed, transmission speed, wheel speed and the engine map. Therefore all signals required for parameter estimation are already available. Data acquisition is carried out in the Matlab/Simulink environment using DSpace real time prototyping hardware. The data was captured at 100 Hz to obtain reliable modeling of upto 10 Hz dynamics. This captures the first major resonance of the driveline dynamics and is adequate for launch control design purposes.

C. Data Analysis

The tests were run by providing step torque inputs to the drive-line with the master clutch locked. Three tests were carried out on the same route. Analysis of the data reveals that firstly, transmission and engine speeds match closely, hence that junction is stiff. This is validated by the fact that there were no torsional springs in the clutch. Secondly, there is significant compliance in the driveline downstream of the transmission to the wheel. The first major vibration mode, which is 1.5 Hz to 2 Hz is seen clearly and is characterized by large torsional displacements and torque amplitudes.

D. Parameter Estimation

Parameter estimation using Matlab is performed as follows. A simulator for the locked clutch model is used to compute the engine and wheel speeds. The unconstrained minimization procedure that is included in Matlab optimization toolbox (`fimunc`) is used to minimize the error between calculated and measured values of the engine and wheel speeds. The error function is expressed as

$$\epsilon^2 = \sum_{all\ i} \left(\left(\alpha_w^{meas} - \alpha_w^{cal}\right)^2 + \left(\frac{\alpha_e^{meas}}{n} - \frac{\alpha_e^{cal}}{n}\right)^2 \right) \quad (8)$$

During each iteration of the minimization routine, the A, B, C and D matrices are recalculated from the updated value of the various parameters. The model output is then supplied to the error function to obtain the scalar error. For unbiased perturbation of the variables in order to calculate the gradients, it is important to normalize the variables with respect to their initial guesses. The final estimated values of the parameters are the ones that minimize the error function and satisfy the convergence criteria. The results of the estimated parameters from 3 runs are shown in Table I.

TABLE I

Estimated parameters from runs 1 to 3

Run	**J1** (Nm^2)	**J2** (Nm^2)	**d1** $\left(\frac{Nm}{rad/sec}\right)$	**d2** $\left(\frac{Nm}{rad/sec}\right)$
1	1.34	1949	0.576	8.859
2	1.37	2007	0.719	9.258
3	1.31	1996	0.645	8.744

Run	**d** $\left(\frac{Nm}{rad/sec}\right)$	**K** (Nm)	**l** (Nm)	**n**
1	709	60679	159	32.3
2	1291	54122	155	32.01
3	985	57844	163	32.44

E. Observations

The measured and estimated values for the engine and wheel speeds from run 1 are shown in Fig 1. The estimated parameters with the exception of the damping values, agree reasonably well with physical data. Similar observations were made on runs 2 and 3. Damping parameters are difficult to estimate. The quality of fit is not very sensitive to damping parameters and the estimated parameters do not change significantly with a wide range of damping values. Hence the degree of confidence in estimated damping is lower. The first major resonance of the driveline, which includes low frequency vibration amplitudes is captured by this model. There is an indication that the calculated response in engine speeds has more damping than the actual engine speed. The calculated wheel speed matches quite closely with measured values. Some additional vibration modes are also seen in the calculated response. This could arise from the assumption of a stiff wheel. Additionally, the observed phase shift delay may be explained by the

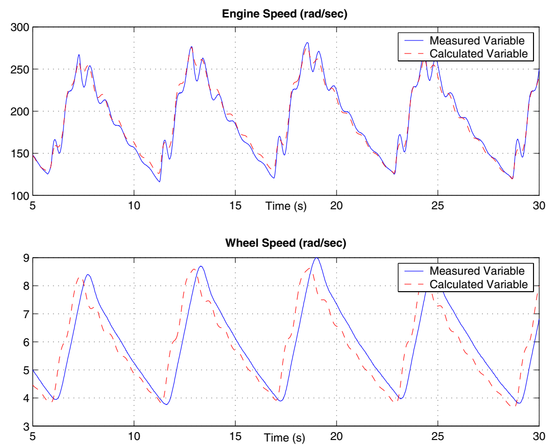

Fig. 1. Comparison of calculated and measured speeds for engine and wheel from run 1.

assumption of stiff clutch and propshaft components. Shaft stiffness is estimated lower than material data. This is a fallout from treating the propshaft as a stiff member.[2] The estimated gear ratio is at least 10 percent higher than the actual ratio. This ratio adjustment has to be made to take into consideration unmodeled dynamics between the transmission output and the wheel. Two important areas of modeling improvement would be to consider a flexible propeller shaft and treat the wheel as a spring element with frictional damping.

V. Controller Design

The main objective of the clutch engagement controller is to ensure a smooth vehicle launch from stationary state. In the absence of an automatic controller, a skilled driver would manipulate the clutch pedal and the accelerator in a manner that launches the vehicle rapidly while minimizing the extent of lurch. There are several key requirements to be considered during the engagement processes. Engaging the clutch too fast during standing starts can result in high acceleration of the driveline and wheels. This may cause undesirable wheel slip and in the extreme case even stall the engine. On the other hand extending the clutch slip duration too long can cause excessive clutch heat build up and premature wear. Another important parameter that defines the engagement quality is the slip acceleration just before lock up. Ideally this acceleration should be zero to prevent driveline torsional excitation. Factors that cause a non-zero slip before lock up would be a rapid clutch acceleration that results in overshoot, and change in friction coefficient during the dynamic-static transition. Therefore in designing the controller, the following performance indices must be satisfied,

- Minimize the clutch lock up time
- Control the clutch lock up behavior to prevent engine droop also known as the no kill criteria
- Control the clutch lock to manage vehicle lurch. Vehicle lurch is the measure of longitudinal acceleration when the clutch goes through lock up. Szadakowski [3] has shown that limiting the acceleration to 0.15 g ensures a comfortable launch
- Minimize the energy dissipated in the clutch during the slipping process

A. Design 1: Clutch Torque as Input

The plant does not have an integrator (type 0 plant) and therefore, to drive the slip speed to zero, an integrator has to be placed in the feedforward path between the error comparator and the plant output. Using ξ as the integrator output, we get

$$\dot{\mathbf{x}} = \mathbf{A}\mathbf{x} + \mathbf{B}u \tag{9}$$

$$y = \mathbf{C}\mathbf{x} \tag{10}$$

$$u = -\mathbf{K}\mathbf{x} + k_i \xi \tag{11}$$

$$\dot{\xi} = r - \mathbf{C}\mathbf{x} \tag{12}$$

where,

$\mathbf{x}$ is the state vector of the plant, u is the control signal
y is the output signal, r is the reference input

Subtracting steady state values indicated by the subscript ss, and introducing

$$x_e(t) = x(t) - x(ss)$$
$$\xi_e(t) = \xi(t) - \xi(ss)$$
$$u_e(t) = u(t) - u(ss)$$

equations (9) to (12) can be written as

$$\begin{pmatrix} \dot{\mathbf{x}}_\mathbf{e}(t) \\ \dot{\xi}_e(t) \end{pmatrix} = \begin{pmatrix} \mathbf{A} & 0 \\ -\mathbf{C} & 0 \end{pmatrix} \begin{pmatrix} x_e(t) \\ \xi_e(t) \end{pmatrix} + \begin{pmatrix} \mathbf{B} \\ 0 \end{pmatrix} u_e(t) \tag{13}$$

where,

$$u_e(t) = -\mathbf{K}\mathbf{x}_\mathbf{e}(t) + k_i \xi_e(t) \tag{14}$$

Therefore equations 13 and 14 can be represented as

$$\dot{\mathbf{e}} = \hat{\mathbf{A}}\mathbf{e} + \hat{\mathbf{B}}\mathbf{u}_\mathbf{e} \tag{15}$$

where

$$\mathbf{e}(t) = \begin{pmatrix} x_e(t) \\ \xi_e(t) \end{pmatrix} \qquad \hat{\mathbf{A}} = \begin{pmatrix} \mathbf{A} & 0 \\ -\mathbf{C} & 0 \end{pmatrix}$$

$$\hat{\mathbf{B}} = \begin{pmatrix} \mathbf{B} \\ 0 \end{pmatrix} \qquad u_e = -\hat{\mathbf{K}}\mathbf{e}$$

$$\hat{\mathbf{K}} = [\mathbf{K} \ \ -k_i]$$

The optimal control strategy involves calculating the control vector, $\mathbf{u(t)}$, which minimizes a given performance index. If the performance index is a quadratic function, then the minimization results in a linear control law given by

$$\mathbf{u}(t) = -\mathbf{K}\mathbf{x}(t) \tag{16}$$

[2]As pointed out by one of the reviewers of this paper, the phase shift may also be caused from drivetrain back-lash which can be significant

TABLE II

PERFORMANCE INDEX CONSTANTS AND THE RESULTING OPTIMAL GAINS FOR EACH CASE USING DESIGN 1 LQR CONTROLLER

Case	Weighting Factors		Optimal Gains				
	β	r_0	**K1**	**K2**	**K3**	**K4**	**K5**
1	0.2	1.45	-0.48	-3.60	0.32	19.73	0.37
2	0.2	0.50	-0.89	1.11	0.71	25.99	0.63
3	0.3	0.10	-2.23	79.58	2.19	35.29	1.73
4	0.4	0.05	-3.28	197.82	3.37	39.60	2.83
5	0.6	0.01	-7.62	-1010.7	8.26	60.87	7.74

The performance index, can be written as

$$J = \int_0^\infty \left(\mathbf{x^T Q x} + \mathbf{u^T R u} \right) dt \tag{17}$$

where $\mathbf{Q}$ and $\mathbf{R}$ are both positive definite Hermitian or real symmetric matrices. The first term represents cost of the state vector error, whereas the second term represents cost of the control signal. The minimization of this equation, is carried out by solving Riccatti's continuous time equation, which in turn yields the optimal feedback gains, $\mathbf{K}$ which is a r x n matrix. The matrix Q and R is written as

$$Q = \text{diag}\left(\begin{bmatrix} 1 & 1 & 1 & 1000 & \beta \end{bmatrix} \right)$$
$$R = r_0$$

where, `diag` represents the diagonal elements of the matrix Q, β is the weighting factor on the slip speed and r_0 is the weighting factor on the input. The LQR controller design is based on the plant generated from run 1 shown in Table I. The optimal gains are calculated by using Matlab's `lqr` function. 5 sets of the weighting factors are chosen such that for each case, a smooth overdamped lock up is obtained. Fig 2 shows the clutch torque, slip speed and longitudinal acceleration for the 5 cases. For each case, the weighting factors and the corresponding optimal gains are shown in Table II and the various clutch engagement performance parameters are shown in Table III.

TABLE III

PEAK CLUTCH TORQUE, PEAK LONGITUDINAL ACCELERATION AND PEAK POWER FOR VARIOUS LOCKUP TIMES USING CLUTCH TORQUE INPUT IN DESIGN 1 LQR CONTROLLER

Case	LockUp Time (sec)	Peak Clutch Torque (Nm)	Peak Acceleration (g)	Peak Power (KW)
1	1.95	609	0.29	48.8
2	3.3	262	0.21	20.9
3	4.8	178	0.17	14.3
4	7.75	75	0.08	5.77
5	9.74	59	0.04	3.47

B. Design 2: Clutch Torque Rate as Input.

The next step is to introduce another state variable, namely clutch torque, since in reality, the driver controls the clutch torque by changing the rate at which he manipulates the clutch force via the clutch pedal. The development of the state space matrices follows the same differential equations described in Section III with the additional state to represent the clutch torque. Define

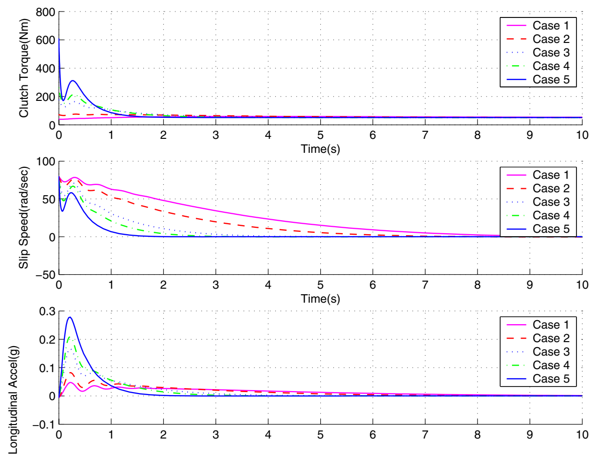

Fig. 2. Plots of clutch torque, slip speed and longitudinal acceleration using clutch torque input with various targeted slip times using design 1 LQR controller

$$x_5 = T_c \tag{18}$$

Let x_5 be the input to clutch system. Therefore

$$\dot{x_5} = u_c \tag{19}$$

where u_c is the clutch torque rate. The state matrices can now be expressed as Using the same definitions of J_0, J_1, J_2, b_1, b_2 and T_l as described earlier, with additional substitution as follows

$$b_3 = b_1 + \frac{b_a}{n^2} \qquad b_4 = b_a + b_2 \tag{20}$$

$$\mathbf{A_s} = \begin{pmatrix} -\frac{b_e}{J_0} & 0 & 0 & 0 & -\frac{1}{J_0} \\ 0 & 0 & \frac{1}{n} & -1 & 0 \\ 0 & -\frac{K_a}{nJ_1} & -\frac{b_3}{J_1} & \frac{b_a}{nJ_1} & \frac{1}{J_1} \\ 0 & \frac{K_a}{J_2} & \frac{b_a}{nJ_2} & -\frac{b_4}{J_2} & 0 \\ 0 & 0 & 0 & 0 & 0 \end{pmatrix}$$

$$\mathbf{B_s} = \begin{pmatrix} \frac{1}{J_0} & 0 & 0 \\ 0 & 0 & 0 \\ 0 & 0 & 0 \\ 0 & -\frac{1}{J_2} & 0 \\ 0 & 0 & 1 \end{pmatrix} \qquad \mathbf{U_s} = \begin{pmatrix} T_e \\ T_l \\ u_c \end{pmatrix} \tag{21}$$

The control objective consists of minimizing the slip time, dissipated power and the slip acceleration just prior to lock up, the performance index stated in (17) is modified as follows, to include these minimization parameters.

$$J = \frac{1}{2} \int_0^\infty \left(\alpha s T_c + \beta s^2 + \gamma \dot{s}^2 + r u^2 \right) dt \tag{22}$$

where,
T_c is the clutch torque, s is the clutch slip speed
α is the weighting factor for clutch power
β is the weighting factor for slip speed
γ is the weighting factor for slip acceleration
Introduce the following substitutions,

$$C_1 = \begin{bmatrix} 1 & 0 & -1 & 0 & 0 \end{bmatrix}$$
$$C_2 = \begin{bmatrix} 0 & 0 & 0 & 0 & 1 \end{bmatrix}$$
$$Q = \alpha \frac{C_1^T C_2 + C_2^T C_1}{2} + \beta C_1^T C_1 + \gamma A^T C_1^T C_1 A$$
$$N = \gamma A^T C_1^T C_1 B$$
$$R = r + \gamma B^T C_1^T C_1 B$$

Inserting these in (22) the performance index for the optimal control with clutch torque rate as the input is written as

$$J = \frac{1}{2} \int_0^\infty \left(x^T Q x + 2x^T N u + R u^2 \right) dt \qquad (23)$$

The Q, N and R matrices are tuned individually by changing the various weighting factors for each matrix, to give the desired overdamped clutch response. As in design 1, the plant derived from run 1 in Table I is used for controller design. Fig 3 shows the clutch torque, slip speed and longitudinal acceleration for the 5 cases, where each case represents a certain lock up behavior. Tables IV and V shows the performance index constants α, β and γ used for each case and the corresponding optimal gains obtained. Table VI shows the various clutch engagement performance parameters for each test.

TABLE IV
PERFORMANCE INDEX CONSTANTS FOR DESIGN 2 LQR CONTROLLER

Case	Performance Indices		
	α	β	γ
1	0	20	1
2	0	45	50
3	0	160	300
4	1	300	650
5	20	1020	2800

TABLE V
OPTIMAL GAINS FOR EACH RUN OF DESIGN 2 LQR CONTROLLER

Case	Optimal Gains					
	K1	**K2**	**K3**	**K4**	**K5**	**K6**
1	-1.13	-188.39	0.542	89.70	2.33	1.41
2	-1.70	-367.52	0.796	123.30	2.84	2.23
3	-3.7	-1327.8	1.9	219.6	4.3	5.5
4	-5.1	-2289.4	3.0	273.4	5.3	8.1
5	-9.5	-5938.5	7.9	367	8.1	16.7

VI. CONCLUSIONS

1) Estimated driveline parameters matched reasonably well with physical data and first major resonance in the driveline is captured by the model. A phase shift in the calculated wheel speed may be due to stiff clutch and propshaft assumptions. The unmodeled dynamics between transmission output and wheel speed may explain the higher estimated gear ratio.
2) From the two optimal control strategies, a comparison of the critical performance parameters is made. Fig 4, shows the comparison of the longitudinal acceleration. It is clear that the design 2 LQR controller gives the smoothest launch with peak acceleration of 0.12g for 2.5 sec lock up compared to the more than 0.25g for the other controller.
3) From Fig 5, it is seen that lower peak clutch torque is obtained for design 2 LQR controller for lock up duration less than 3.5 sec. At higher lock up times, the trend is reversed.
4) The comparison of the peak clutch power in Fig 6 which directly relates to clutch life, shows at lower lock up time, the design 2 LQR controller dissipates lesser peak power. Thus the design 2 LQR controller shows good performance characteristics for lock up times of 3.5 secs and lower when compared to the other controller. A stable and smooth launch can be expected with this control strategy.
5) The design 2 LQR controller gives a high degree of

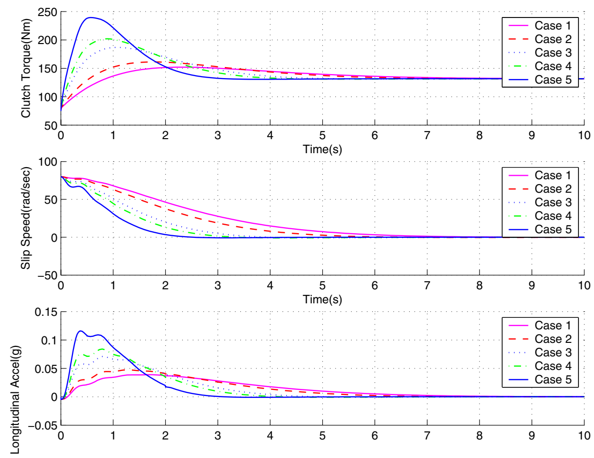

Fig. 3. Plots of clutch torque, slip speed and longitudinal acceleration using clutch torque rate input optimal controller (design 2) with various targeted slip times. Clutch torque rate is the input

TABLE VI
PEAK CLUTCH TORQUE, PEAK LONGITUDINAL ACCELERATION AND PEAK POWER FOR VARIOUS LOCKUP TIMES USING CLUTCH TORQUE RATE INPUT, DESIGN 2 LQR CONTROLLER

Case	**LockUp Time** (sec)	**Peak Clutch Torque** (Nm)	**Peak Acceleration** (g)	**Peak Power** (KW)
1	2.5	239	0.12	15.1
2	3.40	201	0.08	12.7
3	4.00	187	0.07	11.6
4	6.30	161	0.04	9.8
5	8.40	151	0.04	9.32

flexibility to the user to select a particular vehicle launch profile. This is done in practice, by changing the weighting factors and thereby using a new set of controller gains with the use of lookup tables. For example if a very aggressive launch is required then from Table VI it is seen that case 1 gives a lockup time of 2.5 sec. Referring to Tables IV and V, the corresponding performance indices for α, β, γ and the optimal gains $K1$ through to $K6$, are used in the controller. On the other hand if a more comfortable launch is desired then the controller parameter corresponding to a lock up time of 4 sec could be used. Here the peak acceleration is much lower compared to the aggressive launch case. In situations like hill start where very aggressive launch is necessary, the parameters can be taken in from design 1 controller. Case 3, as shown in Tables II and III for instance, can provide very high starting clutch torque while keeping the peak acceleration within acceptable bounds. The options for various engagement types can be provided in the form of driver selectable switches, where each switch corresponds to a unique set of clutch engagement tuning parameters.

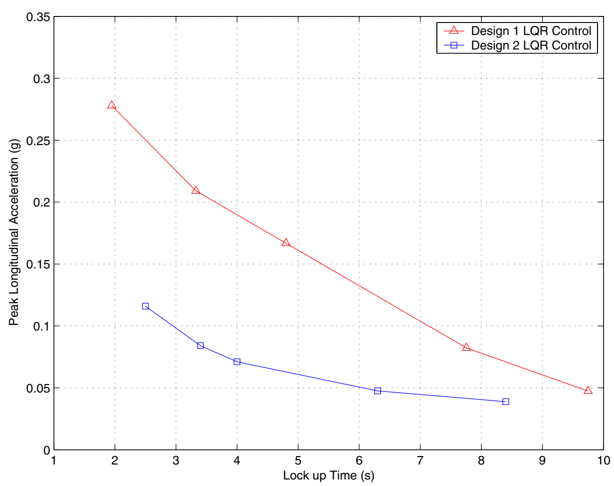

Fig. 4. Comparison of longitudinal acceleration using the 2 LQR controllers

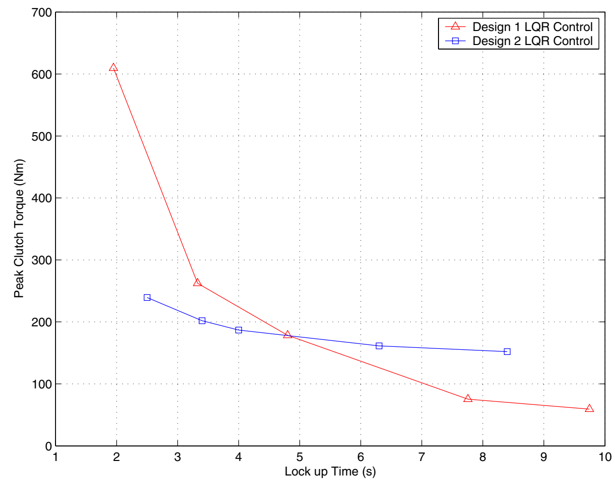

Fig. 5. Comparison of peak clutch torque using the 2 LQR controllers

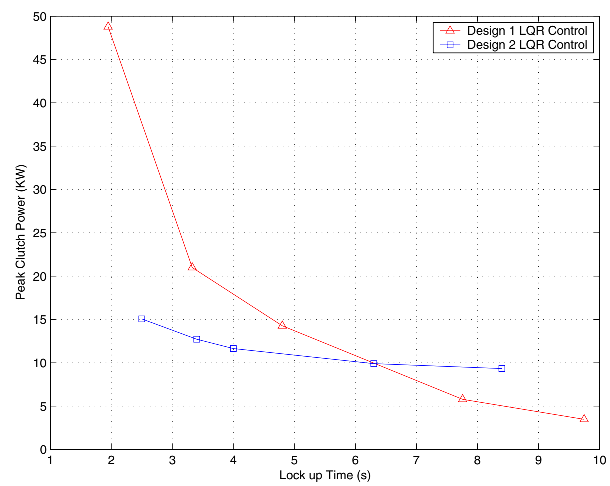

Fig. 6. Comparison of peak clutch power using the 2 LQR controllers

REFERENCES

[1] Tanaka, H., [1981], Electro- Pneumatically Operated Proportional Clutch for Semi-Automatic Power Transmission. JSAE Review, No. 5, pp 31-36.

[2] Sumida, S. and Nobumoto, K., [1985], Vehicle Startup Control System Using Friction Clutch. JSAE Review, April, pp 48 to 58.

[3] Szadkowski, A. and Morford, R.B., [1992], Clutch Engagement Simulation: Engagement Without Throttle. SAE Technical Paper 920766.

[4] Szadkowski, A. and McNerney, G. J., [1992], Clutch Engagement Simulation: Engagement With Throttle. SAE Technical Paper 922483.

[5] Nordgard, K. and Hoonhorst, H., [1995], Developments in Automated Clutch Management Systems. SAE Technical Paper 950896.

[6] Tanaka, H. and Wada, H., [1995], Fuzzy Control of Clutch Engagements for Automated Manual Transmission. Vehicle System Dynamics, 24, pp. 365-376.

[7] Wu, G., Shen, S. and Yan, G., [1997], Stability Analysis for Fuzzy Control of Clutches, SAE Technical Paper 972773.

[8] Chen, L., Jianwu, Z. and Weigang, H., [1999], Feedback Linearization Control for Electronically Controllable Clutch of Vehicle. Chinese Journal of Mechanical Engineering, Vol. 12, No. 4.

[9] Hibino, R., Osawa, M., Yamada, M., Kono, K. and Tanaka, M., [1996], Control Design for Torque-Converter-Clutch Slip System. Proceedings of the Conference of Decision and Control, 1996, Kobe.

[10] Slicker, J. and Loh, R.N.K., [1996], Design of Robust Vehicle Launch Control System. IEEE Transactions on Control Systems Technology, Vol.4, No.4, July.

[11] Glielmo, L. and Vasca, F., [2000], Optimal Control of Dry Clutch. SAE Technical Paper 2000-01-0837.

[12] Garofalo, F., Glielmo, L. Iannelli, L. and Vasca., [2002], Optimal Tracking for Automotive Dry Clutch Engagement. 15th Triennial World Congress, IFAC, 2002, Barcelona, Spain,

[13] Pettersson, M. [1996], Driveline Modeling and Principles for Speed Control and Gear Shift Control. Linkoping Studies in Science and Technology, Thesis No.564, Linkoping 1996.

A. List of Symbols

T_e	Engine torque
T_c	Clutch torque
T_t	Transmission torque reflected to input
T_p	Propeller shaft torque
T_f	Final Drive torque reflected to input
T_a	Axle shaft torque
T_w	Wheel torque
J_e	Engine flywheel and clutch input inertia
J_t	Transmission inertia reflected to output
J_f	Final Drive inertia reflected to output
J_w	Wheel inertia
α_e	Engine flywheel angular dispalcement
α_{c1}	Clutch input angular dispalcement
α_{c2}	Clutch output angular dispalcement
α_c	Clutch angular dispalcement
α_t	Transmission output angular dispalcement
α_p	Propeller shaft output angular dispalcement
α_f	Final Drive shaft output angular dispalcement
α_w	Wheel angular dispalcement
b_e	Flywheel and clutch input damping
b_t	Transmission damping reflected to output
b_f	Final Drive damping reflected to output
b_a	Axle shaft internal structural damping
b_w	Wheel damping
n_t	Transmission ratio
n_f	Final Drive ratio
K_a	Axle shaft torsional stiffness
m	Mass of vehicle
g	Gravity constant
v	Linear velocity of vehicle
F_w	Driving wheel force
F_a	Air drag force
F_r	Rolling resistance
F_g	Graviational force
c_w	Air drag coefficient
A_a	Frontal area
ρ_a	Air density
c_{r1}	Tire slip coefficient 1
c_{r2}	Tire slip coefficient 2
ξ	Road gradient